

In situ sampled snow particle sizes of the East Antarctic ice sheet and their relation to physical and remotely sensed snow surface parameters

Susanne INGVANDER,¹ Helen E. DAHLKE,¹ Peter JANSSON,¹ Sylviane SURDYK²

¹Department of Physical Geography and Quaternary Geology, Stockholm University, Stockholm, Sweden
E-mail: susanne.ingvander@natgeo.su.se

²National Institute of Polar Research, Research Organization of Information and Systems, Tachikawa, Tokyo, Japan

ABSTRACT. Knowledge of snow properties across Antarctica is important in estimating how climate could potentially influence the mass balance of the Antarctic ice sheet. However, measuring these variables has proven to be challenging because appropriate techniques have not yet been developed and extensive datasets of field estimates are lacking. The goal of this study was to estimate the relationship between field-observed snow particle-size parameters from across the East Antarctic ice sheet and a suite of spatial datasets (i.e. topography, remote-sensing data) using a principal component analysis (PCA). Five snow particle-size parameters were correlated to spatial datasets of the following five groups: (1) relief properties such as elevation and slope; (2) remote-sensing data from Moderate Resolution Imaging Spectroradiometer (MODIS) and synthetic aperture radar (SAR) sensors; (3) spatially interpolated data (i.e. 10 m maps of temperature and approximate snow accumulation in $\text{kg m}^{-2} \text{a}^{-1}$); (4) field-retrieved data on surface roughness; and (5) in situ elevation and distance from the coast. The results show that the relief parameter slope correlated best with the snow particle length and area ($r=0.76$, $r=0.80$). Further, the PCA indicated that the different remote-sensing parameters correlated differently with the size parameters and that the most common parameter in visual analysis, particle length (grain diameter), is not always the optimal parameter to characterize the snow particle size as, for example, area correlates better to slope and aspect than length.

INTRODUCTION

Ice sheets play an important role in the Earth's climate system and water cycle. Antarctica stores ~70% of the Earth's fresh water. It is therefore of interest to understand the present state of the East Antarctic ice sheet (EAIS) to estimate future changes in its surface mass balance (Lemke and others, 2007). However, estimating the mass balance of the EAIS remains a challenge. The most applicable method for studying such extensive areas as ice sheets is using active and passive remote sensing such as radar or laser altimetry (Zwally and others, 2005; Wingham and others, 2006) or optical satellite images such as the Mosaic of Antarctica (MOA; Scambos and others, 2007). Several different sensors such as the Cryosat-2 (Drinkwater and others, 2004) are available to monitor the EAIS regularly. In order to accurately interpret remotely sensed information on snow, ground observations and in situ measurements are needed that capture the spatial heterogeneity of snow properties over vast areas such as the EAIS. Traverse expeditions provide a unique opportunity to collect ground-truth data for validation of remotely sensed data on snow properties. However, validation of remotely sensed data on snow properties in remote areas such as the EAIS is often limited by the availability of field-observed snow properties that cover large areas and the temporal validity of both the field-observed snow properties and the remote-sensing data since snow conditions can change quite rapidly.

The surface snow conditions in Dronning Maud Land (DML), part of the EAIS, have been of interest and under investigation since the 1950s (Liljequist, 1957). As early as 1955, Schytt investigated snow accumulation patterns, snow albedo and snow particle size on the EAIS (Schytt, 1958).

During the International Polar Year (2007–09), the Japanese–Swedish Antarctic Expedition (JASE) 2007–08 traversed the EAIS (Fujita and others, 2011), which provided a unique opportunity to investigate snow properties such as snow particle size and snow surface hardness across a large area. The motivation for determining these snow properties along the route was to aid the interpretation of remote-sensing data since parameters such as snow particle size strongly affect the scattering properties of the snowpack and the reflectivity from the snow surface (Wiscombe and Warren, 1980; Ulaby and Dobson, 1989; Fierz and others, 2009). The effect on scattering properties requires sound knowledge of snow particle-size parameters to correctly interpret synthetic aperture radar (SAR) data (Shi and Dozier, 2000). Furthermore, Wiscombe and Warren (1980) showed that an increase in snow particle size reduces the albedo of the snow surface, which in turn strongly affects the energy budget of the Earth's surface (Lemke and others, 2007).

The objective of this study was to evaluate different spatial datasets such as remote-sensing and topography-derived data for their usability to extrapolate point information of field-observed snow particle-size data. Our hypothesis is that the topographic characteristics of DML will affect the correlation between our spatial datasets and the data on snow particle sizes. Here the term 'snow particle' is used because the applied field method for estimating size, area and shape metrics of snow grains does not support the distinction between polygranular crystals and polycrystalline grains (i.e. essentially single crystals from aggregated crystals; Sommerfeld and LaChapelle, 1970). The objective of this study is motivated by the need to extend the existing body of studies that validate remote-sensing data of snow

Table 1. Group, type of data, sensor, spatial resolution, data source and acquisition date and reference for the spatial datasets used in the statistical analysis performed in this study. The datasets are provided by the RADARSAT-1 Antarctic Mapping Project (RAMP), the British Antarctic Survey (BAS) and the US National Snow and Ice Data Center (NSIDC). The sensors used are the European Remote-sensing Satellite-1 (ERS-1), MODIS, RADARSAT SAR, the Advanced Microwave Scanning Radiometer for Earth Observing System (AMSR-E) and the Advanced Very High Resolution Radiometer (AVHRR). Two of the overarching projects are MOA and THERMAP

Group	Datasets	Sensors/project	Spatial resolution	Data source and acquisition date	Reference
1	Elevation	ERS-1–ICESat	1 × 1 km ²	ERS-1 (Mar 1994), ICESat (2003–08)	Bamber and others (2009)
	Slope	ERS-1–ICESat	1 × 1 km ²	ERS-1 (Mar 1994), ICESat (2003–08)	Bamber and others (2009)
	Aspect	ERS-1–ICESat	1 × 1 km ²	ERS-1 (Mar 1994), ICESat (2003–08)	Bamber and others (2009)
2	MOA	MODIS	125 m (5 × 5 pixels interpolated grid)	NSIDC (Nov 2003–Feb 2004)	Haran and others (2005)
	SAR 125 m	RADARSAT SAR	125 m (5 × 5 pixels interpolated grid)	RAMP (1 Sept 1997 to 31 Oct 1997)	Jezek and others (2002)
	SAR 25 m	RADARSAT SAR	25 m	RAMP (1 Sept 1997 to 31 Oct 1997)	Jezek and others (2002)
3	Approximate snow accumulation	AMSR-E, AVHRR	100 km	BAS (calculated annual accumulation rate)	Arthern and others (2006)
	10 m snow depth temperature	THERMAP	Extrapolated point data	NSIDC (1949–79)	Bohlander and Scambos (2001) and in situ data
	Relative grain size	MOA – snow grain-size product	750 m	NSIDC (Nov 2003–Feb 2004)	Haran and others (2005)
4	Surface roughness	–	–	In situ measurement (Nov 2007–Feb 2008)	In situ data
	Snow resistance	–	–	In situ measurement (Nov 2007–Feb 2008)	In situ data
5	GPS elevation	GPS	<15 m accuracy on 95% typical	In situ registration (Nov 2007–Feb 2008)	In situ data
	Distance from coast	–	–	Calculated by 72° S – GPS position	Calculated

with field-measured data on snow properties. As such, the snow particle-size parameters used in this study are interpreted as a measure for characterizing the scattering body of radiation (Nagler and Rott, 2000). For the study we tested five different groups of spatial data: (1) relief properties such as elevation, slope and aspect; (2) remote-sensing data from Moderate Resolution Imaging Spectroradiometer (MODIS) and SAR sensors (see Table 1 for specification); (3) spatially interpolated data (i.e. 10 m maps of snow temperature and approximate snow accumulation); (4) field-retrieved data on surface properties; and (5) in situ elevation and distance from the coast. In order to determine spatial datasets that reflect the observed differences in snow particle size, the available datasets from each group were first correlated with each of the five snow particle-size parameters. A principal component analysis (PCA) was then conducted to identify structure and redundancy among the size parameters and spatial datasets and to identify the snow particle-size parameters that correlated best with the various spatial datasets. Such information potentially could be helpful to better quantify snow properties in remote areas and to improve snow indices derived from remote-sensing data. It could also be used for interpolation purposes.

METHODS

The material for this analysis is based on data collected during the 2007/08 JASE traverse in DML (Fujita and others, 2011). During the Swedish part of JASE, surface snow, defined as the topmost 1 cm of the snowpack, was sampled at

62 sites along the 1800 km route from the coastal Swedish station (73°04' S, 13°41' W) to the meeting point with the Japanese expedition team (75°89' S, 25°83' W). The locations of the 62 sampling points were randomly selected, but were determined overall by logistical stops during the expedition (Fig. 1). The distance between each sampling site was ~50 km. During each stop along the traverse, a snow sampling site was randomly selected ~20 m away from the expedition vehicles in the windward direction to ensure that the snow surface samples were not influenced by the traverse tracks or vehicle exhaust. At each site a GPS point was taken using a GPS device (Garmin GPS-60, accuracy <15 m, 95% typical) in order to extract information from remotely sensed data (groups 1–3; Table 1) and terrain data observed during the traverse at each site (groups 4–5; Table 1).

At each sampling point, five different snow particle-size parameters were estimated from a digital photograph of a snow sample on a micrometer-accurate reference plate. This method has several advantages: the equipment needed to estimate the snow particle-size parameters is quick to assemble and robust to the varying weather conditions, and the snow particle information collected at a certain location is preserved and available for later reanalysis. The snow particle size was then estimated from the digital photograph using the Digital Snow Particle Property (DSPP) method described by Ingvander and others (2012). The DSPP method is based on previous methods for determining snow particle sizes such as those by Gay and others (2002) and Kärkäs and others (2002). The DSPP method was developed as a robust and quick field method that supports existing visual methods

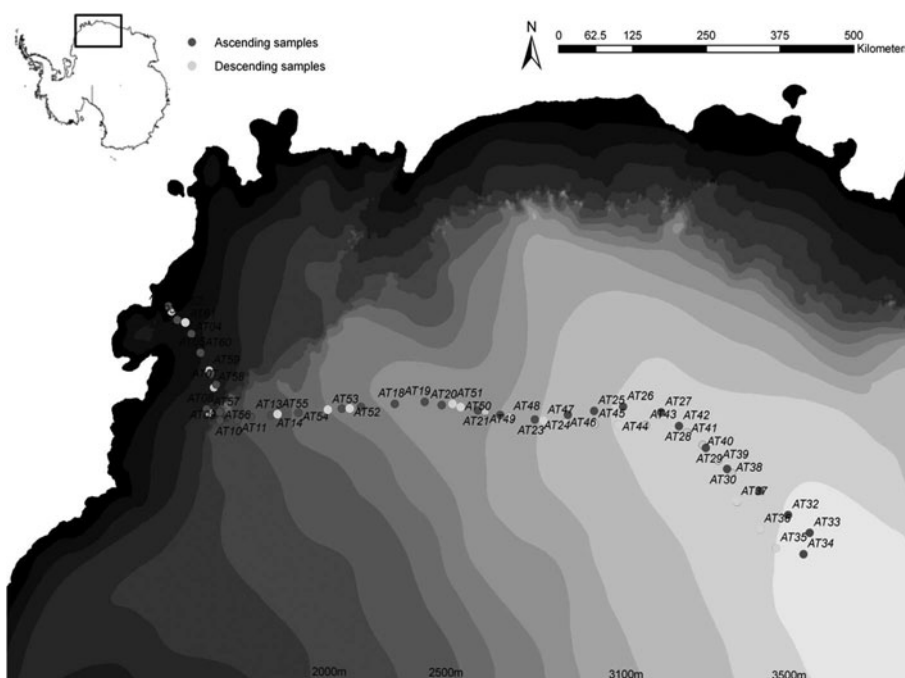


Fig. 1. Surface sample sites during the JASE traverse 2007/08 overlying a topographic map of Antarctica. Dark grey circles are the ascending samples from Wasa to the meeting point, and light grey circles are the descending sample sites on the return to Wasa station. AT numbers indicate the ID of each sample point.

used to interpret snow particle-size parameters in the field. However, this method does not aim to achieve the level of detail and precision provided by tomography analysis or specific surface area estimates (e.g. Matzl and Schneebeli, 2006; Domine and others, 2008; Gallet and others, 2009; Picard and others, 2009). Comparisons have shown that visual methods generally report larger particle sizes than optic equivalent measurements (Aoki and others, 2000).

The DSPP method allows the estimation of two-dimensional size parameters of a snow particle using object-oriented image analysis on the digital photograph of a snow sample. The image resolution in the analysis is 0.03 mm, and the smallest detectable objects have an area of 0.015 mm² (based on image classification lower limit for area set to exclude millimetre markers but detect all larger objects). The object-oriented image analysis generates multiple size parameters by segmenting the image based on shape and colour compactness. The segmented images are then classified into 'snow particle' and 'no snow particle' areas using thresholds for the brightness (to distinguish bright snow particles from the dark-coloured reference plate), the snow particle area (the area threshold excludes reflections from the sample glass, large grain clusters and the millimetre marker reflections) and the snow particle shape (i.e. excluding elongated shapes that are generally produced by reflections in the sample glass). The size parameters retrieved from each image and used in this study are the length (greatest extension of the particle), the width (perpendicular to the length axis), the area (the area of the particle side that is facing the camera calculated using the pixel size multiplied by the number of pixels included in each particle), the largest enclosed ellipse (LEE; i.e. the radius of the largest ellipsoidal feature enclosed by the particle) and the shape (i.e. the length/width ratio) (Ingvander and others, 2011).

Each of the five snow particle-size parameters was correlated to different spatial datasets. For this study, these

spatial datasets are divided into five groups based on the origin and information type of the data (Table 1):

Group 1 – relief properties including: (1) a digital elevation model (DEM) of the surface elevation (m) with a spatial resolution of 1 km, which was derived from European Remote-sensing Satellite-1 (ERS-1) and Ice, Cloud and land Elevation Satellite (ICESat) data (Bamber and others, 2009); (2) the slope (°) derived from the 1 km DEM of the surface elevation; (3) the aspect (i.e. downslope azimuth direction) derived from the 1 km DEM of the surface elevation.

Group 2 – remotely sensed products that constitute images acquired with passive and active sensors: (1) MOA, a composite map (260 images collected during 2003–04) of the roughness of the snow surface of Antarctica produced in 2004 by combining the visible and near-infrared (NIR) bands from the MODIS sensor (Haran and others, 2005); (2) RADARSAT SAR Antarctic mosaic from the RADARSAT-1 Antarctic Mapping Project (RAMP) with a spatial resolution of 125 m (Jezek and others, 2002) representing calibrated radar backscatter data that reflect differences in the surface roughness, dielectric properties and the particle size of the snow; (3) RADARSAT SAR Antarctic mosaic from the RAMP with a spatial resolution of 25 m representing the same properties as the 125 m product.

Group 3 – remotely sensed snow properties derived from remote-sensing data using existing algorithms for parameter retrieval: (1) estimated snow accumulation (kg m⁻² a⁻¹) produced by interpolation of field measurements and satellite images from the Advanced Microwave Scanning Radiometer for Earth Observing System (AMSR-E) and Advanced Very High Resolution Radiometer (AVHRR) instruments (Arthern and others, 2006);

Table 2. Correlation coefficients estimated between each snow particle-size parameter and spatial dataset. Correlation coefficients that were significant at the 5% significance level (two-sided *t* test) are highlighted in bold

Group	Dataset	Length	Snow particle-size parameters			
			Width	LEE	Area	Shape
1	Elevation	-0.70	-0.68	-0.06	-0.63	-0.57
	Slope	0.76	0.75	-0.10	0.80	0.46
	Aspect	0.18	0.18	0.10	0.23	0.04
2	MOA	0.02	-0.01	0.17	-0.07	-0.14
	SAR 125 m	-0.22	-0.24	-0.20	-0.23	-0.02
	SAR 25 m	-0.02	-0.03	-0.16	-0.03	0.13
3	Approximate snow accumulation	0.76	0.74	0.09	0.73	0.59
	10 m temperature	0.70	0.69	0.13	0.67	0.51
	Relative grain size	0.46	0.44	-0.07	0.42	0.49
4	Surface roughness	-0.17	-0.16	0.10	-0.16	-0.18
	Snow resistance	0.14	0.17	0.24	0.26	-0.15
5	Elevation	-0.73	-0.71	-0.14	-0.58	-0.53
	Distance from coast	-0.59	-0.58	-0.13	-0.67	-0.41

(2) interpolated map of field-measured snow temperature at 10 m depth using the THERMAP dataset (Bohlander and Scambos, 2001); (3) map of the relative optical grain size retrieved from the MODIS sensor with a spatial resolution of 750 m (Haran and others, 2005).

Group 4 – field-observed snow surface properties retrieved concurrent with the snow particle-size photography for each snow sample site: (1) surface roughness (determined visually based on the microtopography) classified into four groups (a – flat, b – ripples, c – sastrugi crest, d – sastrugi valley); (2) surface resistance subjectively classified into four classes (1 – soft, 2 – semisoft, 3 – hard, 4 – super hard) based on penetration of a spatula handle 1.5 cm in diameter.

Group 5 – field-surveyed terrain parameters derived on the basis of the position of each sample site: (1) elevation measured with a Garmin 60 handheld GPS device (vertical accuracy <15 m) at each sample site; (2) distance from coast calculated by subtracting the latitudinal coordinate from 72° S as a proxy for distance to moisture source.

The Pearson product-moment correlation coefficient, *r*, was estimated for each combination of a spatial dataset and each of the five snow particle-size parameters. In addition, a Pearson (*n*) PCA (Jolliffe, 2002) was performed on all size parameters and spatial datasets.

RESULTS

Correlation analysis

The spatial extent of the in situ measurements used in this analysis covers a distance of 1800 km in DML, and stretches across the coastal region, through a mountain range and up the EAIS plateau. The time period over which the 62 snow samples were taken was 48 days (Fig. 1). Thus, the estimated snow particle-size parameters used in the analysis varied in space and time. The observed snow particle lengths and areas were generally larger in the low-elevation coastal areas than on the EAIS plateau (Fig. 2). Table 2 shows the results of the correlation analysis between the snow particle-size parameters and the evaluated spatial datasets. Of the snow

particle-size parameters, the snow particle length, width and area showed consistently the highest correlation coefficients with the spatial datasets. Of the spatial datasets, groups 1, 3 and 5 showed the best correlation coefficients (Table 2). Within group 1 (elevation properties) the relief slope was significantly correlated to the snow particle length ($r=0.76$), width ($r=0.75$) and area ($r=0.80$). In addition, both the snow particle length and width were significantly correlated to the elevation above sea level ($r=0.70$ and $r=0.68$, respectively), while the aspect showed generally low correlation coefficients (Table 2). Within group 3 (remotely sensed retrieved snow properties) the snow particle length, width and area were significantly correlated to the approximated snow accumulation ($r=0.76$, $r=0.74$ and $r=0.73$, respectively) and the 10 m temperature map ($r=0.70$, $r=0.69$ and $r=0.67$, respectively). Among the field-surveyed terrain parameters (group 5) both the snow particle length and width showed significant correlations to the GPS-measured elevation ($r=-0.73$ and $r=-0.71$, respectively). In addition, the snow particle area was significantly correlated to the distance from the coast. In order to test the correlation between the size parameters (Table 3), length, width, LEE, area and shape were correlated against each other. Significant correlations are found between all size parameters except LEE, which only correlates significantly to shape ($r=0.55$).

Principal component analysis

All size parameters were analysed in a PCA with the spatial datasets of each group. As indicated in Figure 3, the satellite-derived surface elevation and terrain slope, which were both significantly correlated with the snow particle length (Table 2), explain 94% of the variance in the snow particle length. Figure 4 shows that both the distance from the coast and the elevation measured with the handheld GPS device are able to explain 96% of the observed variability in snow particle area. In contrast, spatial datasets from groups 2 and 4, which showed low correlation coefficients for all snow particle-size parameters, were not able to explain more than 75% of the variance in, for example, snow particle area (Fig. 5). In Figures 3 and 4, the geographic zonation in DML is evident in the biplots, but this pattern is not distinguishable in the RAMP-derived datasets (Jezek and others, 2002) in Figure 5.

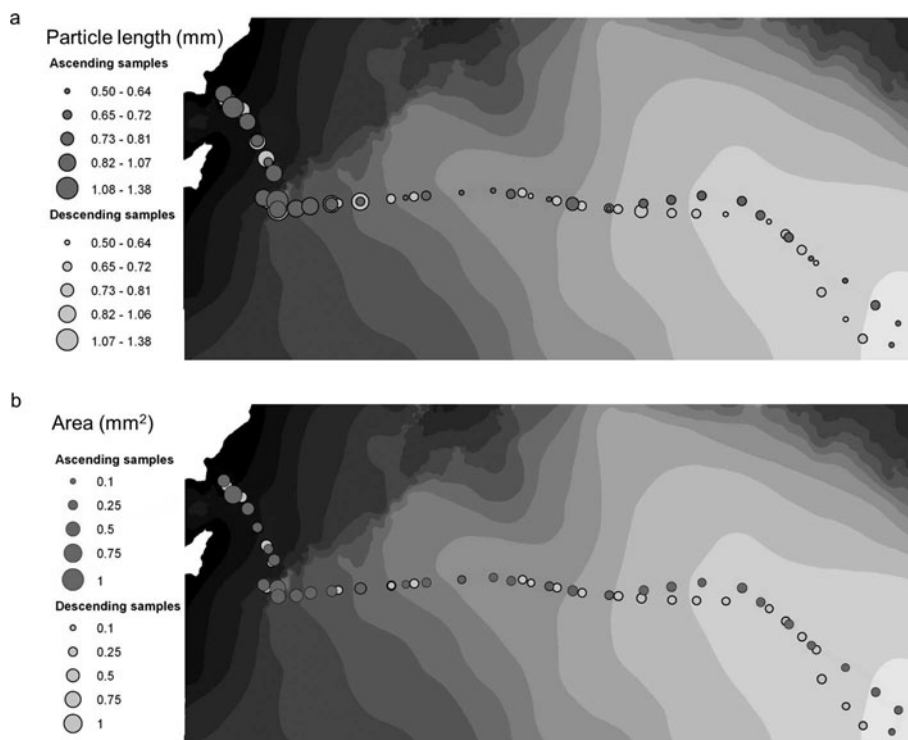


Fig. 2. Two different size parameters: (a) particle length (mm) and (b) area (mm²). The dark grey circles are ascending sample sites and the light grey circles are sample sites on the descent (see Fig. 1; Table 1).

DISCUSSION

The DML landscape is characteristic of Antarctica, with the EAIS plateau connecting to the coastal ice surface by outlet glaciers through the mountain range Heimefrontfjella. The EAIS is connected to the coastal region with ice streams flowing through the transition zone in the mountain range. For all size parameters there is a clear pattern of predominantly smaller particle sizes on the plateau compared with the coastal or transitional region (Fig. 2). This difference can be explained by several physical factors, such as precipitation rate (Arthern and others, 2006), moisture content of the air (Connolley and King, 1993) and air temperature (Connolley and Cattle, 1994), which control the size of a snow particle before deposition on the ground. In addition to these factors, the snow is also subject to redistribution and metamorphic processes that alter the size and shape of snow particles (Stephenson, 1967). However, the degree to which these factors influence snow particle size is determined to a large extent by the topography of

Table 3. Correlation coefficients estimated between the separate snow particle-size parameters. Correlation coefficients that were significant at the 5% significance level (two-sided *t* test) are highlighted in bold

	Length	Width	LEE	Area	Shape
Length		0.93	0.09	0.96	0.69
Width			0.14	0.98	0.65
LEE				0.02	0.55
Area					0.40
Shape					

DML. This is suggested by the fact that all spatial datasets from groups 1 and 5 (i.e. terrain-based data), except for the aspect, are significantly correlated to the snow particle length, width, area and shape (Figs 3 and 4). Both Figures 3 and 4 indicate that there is a clear difference in particle size between the coastal and plateau regions. Our hypothesis was that both aspect and slope of the terrain affect the particle size, but interestingly, based on the results of the PCA, the slope has the strongest effect on particle size. This is particularly apparent in the samples taken in the transition zone (Figs 2 and 3). A potential reason for the high correlation between slope and snow particle size could be that the terrain slope influences the preferential deposition of snow and thus the snow depth and the redistribution and metamorphic transformation of snow by wind (Jaedicke and others, 2000). For example, in the Alps, Lehning and others (2011) found that sheltered areas accumulate more fine particles, while steeper terrain is more exposed to wind and generates more rough snow surfaces. In contrast, the aspect did not show a clear relation to the particle size, as indicated by the correlation analysis (Table 2). This suggests that in DML spatial differences in insolation (i.e. differences in the surface energy balance associated with the differences in aspect) have less influence on the snow particle size and the major effect from insolation comes from the variation in seasonal radiation in Antarctica (Van den Broeke and others, 2005). In addition, the LEE did not show significant correlations to any of the spatial datasets. We hypothesize that this is because the snow particle length, width, area and shape are first-order parameters extracted with the object-oriented image-analysis software (Definiens, 2008), whereas LEE is a calculated parameter determined using an empirical model (Baatz and Schäpe, 2000). Length is the parameter most exposed to change due to metamorphosis (Sommerfeld and LaChapelle, 1970) as it is the longest axis compared

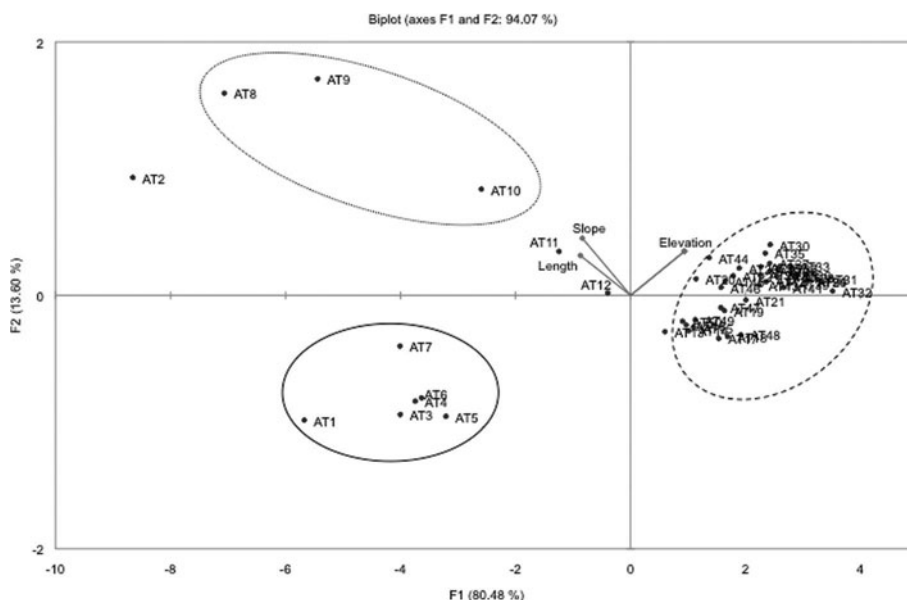


Fig. 3. Biplot of PCA of snow particle length and group 1 (i.e. slope, elevation and interpolated elevation) variables and observations with ID. Geographical clusters are marked with a solid line for coastal samples, a dashed line for plateau samples and a dotted line for the transition zone between the coast and the plateau. AT numbers indicate the sample ID.

with area, being a function of area and width. However, with this investigation unfortunately we cannot identify metamorphic change to the snow particles. Three of the groups (Table 1) showed significant correlations. We have discussed two of them, groups 1 and 5, as direct topographic parameters. The third group with significant correlations is group 3. Group 3 includes spatial datasets that contain parameters which are affected by the topography and distance from the coast, such as the 10m temperatures and the average annual accumulation. These data are closely correlated to temperature and moisture which are governed by elevation and distance from the coast. The EAIS is characterized by topographic properties that affect the climate in the area, which in turn affects precipitation type and amount and, hence, snow particle size (Arthern and

others, 2006; Schlosser and others, 2010). The spatial differences in particle size and their association with different topographic regions have been shown previously by Ingvander and others (2011).

The spatial datasets from group 3 showed significant correlations to the size parameters except for the LEE parameter. The highest correlation coefficient was seen between the particle length and the estimated snow accumulation derived from the model of Arthern and others (2006). This can be attributed to the fact that the coastal areas receive generally higher precipitation amounts in the form of snow due to the proximity to the ocean, which also results in larger snow crystal sizes (Libbrecht, 2005). This is further corroborated by the high correlation coefficients of the particle-size parameters with the interpolated 10m snow

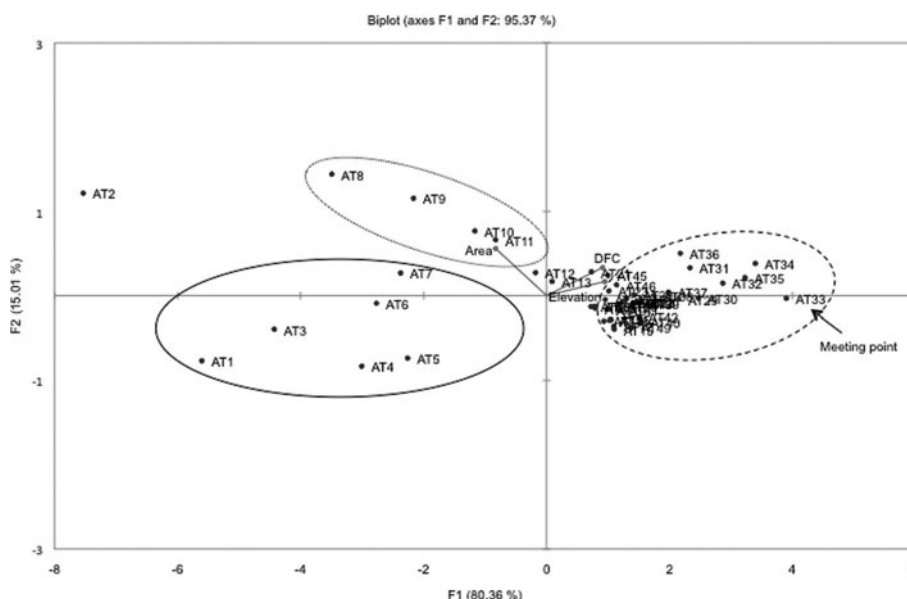


Fig. 4. Same as Figure 3, but for snow particle area and group 5 (i.e. handheld GPS elevation and distance from coast).

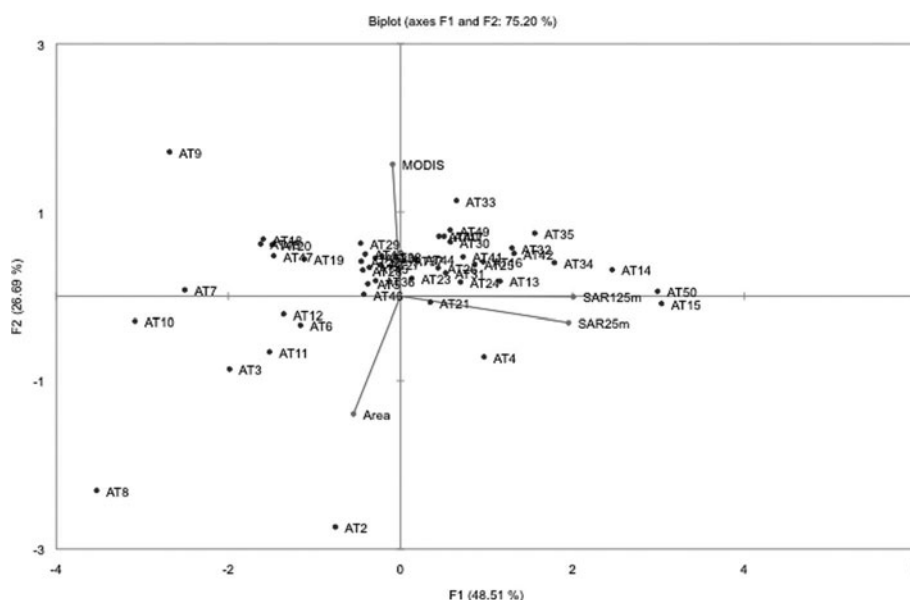


Fig. 5. Biplot of PCA of snow particle area and group 2 (i.e. MOA, SAR 25 m and SAR 125 m) variables and observations with ID. In this biplot the geographical separation is not evident and therefore not marked out. AT numbers indicate the sample ID.

temperature. The 10 m temperature generally reflects the mean annual air temperature of the area (Cuffey and Paterson, 2010), which is also assumed to have a strong effect on the size of the precipitated snow (Libbrecht, 2005). However, the data used here lack information from the Kohnen and Wasa stations (i.e. the transitional and coastal regions), which would probably improve the correlation if it were added.

The correlation coefficients between the snow particle-size parameters and the relative optical snow grain size estimated in the MOA product compiled by Haran and others (2005) varied between $r=0.42$ and $r=0.49$ (except for the LEE parameter which showed $r=-0.07$). We expected that the relative optical snow grain size would show stronger correlation coefficients. However, since the MOA particle-size product was mosaicked from several MODIS images taken in 2003–04 and the field-surveyed particle-size data were sampled during 2007/08, we assume that this correlation coefficient was biased by the large temporal difference between the compared datasets (Scambos and others, 2007).

The remote-sensing-derived datasets in this investigation (groups 1–3) are all derived from compiled products generated as a mosaic of several satellite scenes that were acquired at different times. Thus, these products are temporally not concurrent with the field observations conducted during JASE. However the parameters in groups 1 and 3 are fairly constant (being yearly averages and topographic parameters), so the correlation coefficient is significant. The data in group 2 are also composite products indicating the differences in the surface properties. In group 2, consisting of MOA and RAMP remote-sensing data, we encounter poor correlation. The poor correlation between snow particle size and the RAMP data can be explained by the use of the RADARSAT-1 instrument which operates at C-band (5.3 GHz), penetrating the surface and providing bulk scatter from the snowpack as well as the snow surface (Jezek and others, 2002). The MOA dataset is a mosaic product generated out of 260 MODIS images acquired over 4 months in 2003–04. As the snow particles are subject to change due to metamorphism (Sommerfeld and LaChapelle, 1970), the

temporal difference between the datasets (4 years), the seasonal cycles in insolation (Van den Broeke and others, 2005) and by precipitation (Schlosser and others, 2010), the correlation coefficients in this dataset are also poor.

Furthermore, the snow surface properties observed in situ in group 4 show insignificant correlations to all snow particle-size parameters. This is an unexpected result as the snow surface in Antarctica is highly variable and exhibits a complex pattern of wind-packed areas and accumulation sites. The strong katabatic winds create sastrugi patterns with lee and onward sides that we assumed would show large differences in particle size (Orheim, 1968; Frezzotti and others, 2002). However, the sampling locations used to estimate the snow particle-size parameters were chosen randomly and not with respect to the leeward or windward position relative to sastrugi. Thus, the hypothesized snow particle-size difference associated with the redistribution by wind and preferential deposition cannot be tested sufficiently. These small-scale features need to be studied more closely in the future in order to determine the relationship between the particle size and surface roughness type.

When including several spatial datasets and various snow particle-size parameters within a PCA analysis, it is important to understand the errors introduced by the difference in the spatio-temporal resolution and acquisition date of the spatial datasets, the effect of the topography and also the seasonal evolution of the snow surface. Large seasonal differences in the snow properties in Antarctica are caused by seasonal and diurnal radiation and temperature differences (Van den Broeke and others, 2005), strong coastal winds and more unidirectional wind patterns on the Antarctic plateau (King and Turner, 1997). There are two dominant wind patterns that could influence the snow particle size in the coastal areas and on the polar plateau. At the beginning of the polar summer, katabatic winds transport drier air masses that consist mainly of refrozen evaporated water vapor (diamond dust; Schlosser and others, 2010) from the polar plateau to the coastal areas. During this process, snow particles are likely transported by saltation or suspension (Jaedicke and others, 2000), which could cause

the deposition of smaller snow particles in the transition zone. In contrast, at the end of the austral summer, the predominant wind pattern is from the coastal areas to the polar plateau, which causes an orographic uplift of the moist air masses that precipitates snow particles of approximately the same size both in the transition zone and on the polar plateau. This pattern can be recognized in the spatial datasets in groups 1 and 3, as the parameters in group 1 are based on the topographic features that generate the spatial gradients in DML, whereas group 3 are climate parameters generated as an effect of the topographic features of DML. For example, in group 3 the accumulation distribution is effected by the wind patterns of DML.

The statistical analysis presented in this study is based on a unique snow particle-size dataset collected during JASE 2007/08. However, the results reveal that there is a trade-off when comparing spatial datasets, such as the remote-sensing composite products from groups 1–3, with in situ measurements, especially over such vast regions as Antarctica, as both field data and remote-sensing data are sparse and the collection of field data requires great effort. High correlations were found between spatial datasets and snow particle size which explain the large-scale patterns that are determined by physical factors such as the difference in altitude, air temperature and air moisture. However, field observations and remote-sensing images ideally should be acquired at the same time or within a very short time period. In contrast, the sensitivity of the remotely sensed scattering properties of snow to the snow conditions suggests that remote-sensing products such as the MOA or RAMP mosaic products are of limited use for extrapolating snow particle-size information.

Together these results suggest that more research is needed on the spatio-temporal differences in snow properties. In order to improve the correlation between remote-sensing data and field-observed snow properties, field measurements should be synchronized with the repetition cycle of remote satellite sensors to improve the monitoring of the mass balance of the Antarctic ice shelf.

CONCLUSIONS

Of the snow particle-size parameters considered, the basic size parameters of length, width and area showed significant correlation with most of the spatial datasets derived from surface topography data. The groups of spatial datasets that showed the strongest correlation were those that included data immediately reflecting the topographic features of the region, such as the coastal area, which is separated from the plateau by the transitional zone. Topographically influenced spatial datasets such as the approximate snow accumulation, relative grain size and 10 m snow temperature likewise showed significant correlation coefficients to all snow particle-size parameters. This is because the snow accumulation and temperature are affected by the differences in elevation and the distance from the coast, which in turn affects the snow particle size based on the temperature and moisture content of the air where the snow particles are formed. In DML, the greater the distance from the coast (moisture source) the higher is the elevation. This generates lower temperatures and drier air, and smaller grains are formed than closer to the coast.

In contrast, spatial datasets derived from remote-sensing products such as the MOA and RAMP datasets showed low correlation coefficients to the snow particle-size parameters.

This is due to large temporal differences in the acquisition date of the remote-sensing products and the field-sampled snow particle-size parameters for the MOA data and the issue of subsurface penetration by the RADARSAT-1 sensor in the RAMP. Remotely sensed datasets of less variable data (such as 10 m temperatures and snow accumulation) maintain high correlation to the size parameters, but as the MOA product provides a snow grain-size product on a feature that is highly variable in both time and space, this contributes to the poor correlation between datasets.

ACKNOWLEDGEMENTS

We acknowledge the Swedish Polar Research Secretariat for logistic support and the Swedish Research Council, the National Institute of Polar Research (Japan), the Swedish National Space Board, the YMER-80 Foundation, the Swedish Society for Anthropology and Geography and the Helge Ax:son Johnsons Foundation for financial support. We thank the field crew and staff of both Swedish and Japanese departments who provided the spatial datasets.

REFERENCES

- Aoki T, Fukabori M, Hachikubo A, Tachibana Y and Nishio F (2000) Effects of snow physical parameters on spectral albedo and bi-directional reflectance of snow surface. *J. Geophys. Res.*, **105**(D8), 10219–10236 (doi: 10.1029/1999JD901122)
- Athern RJ, Winebrenner DP and Vaughan DG (2006) Antarctic snow accumulation mapped using polarization of 4.3 cm wavelength microwave emission. *J. Geophys. Res.*, **111**(D6), D06107 (doi: 10.1029/2004JD005667)
- Baatz M and Schäpe A (2000) Multi-resolution segmentation: an optimization approach for high-quality multi-scale image segmentation. In Strobl J, Blaschke T and Griesebner G eds. *Angewandte Geographische Informationsverarbeitung XII*. Wichmann-Verlag, Heidelberg, 12–23
- Bamber JL, Gomez-Dans JL and Griggs JA (2009) *Antarctic 1 km digital elevation model (DEM) from combined ERS-1 radar and ICESat laser satellite altimetry*, National Snow and Ice Data Center, Boulder, CO. Digital media: http://nsidc.org/data/docs/daac/nsidc0422_antarctic_1km_dem/index.html
- Bohlander J and Scambos T (2001) *THERMAP: ice temperature measurements of the Antarctic ice sheet*. National Snow and Ice Data Center, Boulder, CO. Digital media: <http://nsidc.org/data/docs/agdc/thermap/documentation.html>
- Connolley WM and Cattle H (1994) The Antarctic climate of the UKMO unified model. *Antarct. Sci.*, **6**(1), 115–122 (doi: 10.1017/S0954102094000143)
- Connolley WM and King JC (1993) Atmospheric water-vapour transport to Antarctica inferred from radiosonde data. *Q. J. R. Meteorol. Soc.*, **119**(510), 325–342 (doi: 10.1002/qj.49711951006)
- Cuffey KM and Paterson WSB (2010) *The physics of glaciers*, 4th edn. Butterworth-Heinemann, Oxford
- Definiens AG (2008) *Definiens Developer 7 – User Guide*. Definiens AG, Munich
- Domine F and 7 others (2008) Snow physics as relevant to snow photochemistry. *Atmos. Chem. Phys.*, **8**(2), 171–208 (doi: 10.5194/acp-8-171-2008)
- Drinkwater MR, Francis R, Ratier G and Wingham DJ (2004) The European Space Agency's Earth Explorer Mission CryoSat: measuring variability in the cryosphere. *Ann. Glaciol.*, **39**, 313–320 (doi: 10.3189/172756404781814663)
- Fierz C and 8 others. (2009) *The international classification for seasonal snow on the ground*. (IHP Technical Documents in Hydrology 83) UNESCO–International Hydrological Programme, Paris

- Frezzotti M, Gandolfi S, La Marca F and Urbini S (2002) Snow dunes and glazed surfaces in Antarctica: new field and remote-sensing data. *Ann. Glaciol.*, **34**, 81–88 (doi: 10.3189/172756402781817851)
- Fujita S and 25 others (2011) Spatial and temporal variability of snow accumulation in Dronning Maud Land, East Antarctica, including two deep ice coring sites at Dome Fuji and EPICA DML. *Cryos. Discuss.*, **5**(4), 2061–2114 (doi: 10.5194/tcd-5-2061-2011)
- Gallet J-C, Domine F, Zender CS and Picard G (2009) Measurement of the specific surface area of snow using infrared reflectance in an integrating sphere at 1310 and 1550 nm. *Cryosphere*, **3**(2), 167–182 (doi: 10.5194/tc-3-167-2009)
- Gay M, Fily M, Genthon C, Frezzotti M, Oerter H and Winther JG (2002) Snow grain-size measurements in Antarctica. *J. Glaciol.*, **48**(163), 527–535 (doi: 10.3189/172756502781831016)
- Haran T, Bohlander J, Scambos T, Fahnestock M and compilers (2005) *MODIS mosaic of Antarctica (MOA) image map*. National Snow and Ice Center, Boulder, CO. Digital media: <http://nsidc.org/data/nsidc-0280.html>
- Ingvander S, Brown I and Jansson P (2011) Spatial snow grain-size variability along the JASE 2007/2008 traverse route in Dronning Maud Land, Antarctica, and its relation to MOA NDSI index, MEDRIS and MODIS satellite data. In Lacoste-Francis H ed. *Proceedings of ESA Living Planet Symposium: 28 June–2 July 2010, Bergen, Norway*. European Space Agency, Noordwijk
- Ingvander S, Johansson C, Jansson P and Pettersson R (2012) Comparison of digital and manual methods of snow particle size estimation. *Hydrol. Res.*, **43**(3), 192–202 (doi: 10.2166/nh.2012.078)
- Jaedicke C, Thiis TK and Bank B (2000) The snowdrift pattern around a small hill in the high Arctic. In Hjorth-Hansen E, Holand I, Loset S and Norem H eds. *Snow engineering: recent advances and developments. Proceedings of the Fourth International Conference on Snow Engineering, 19–21 June 2000, Trondheim, Norway*. A A Balkema, Rotterdam, 75–80
- Jezek KC and RAMP Product Team (2002) *RAMP AMM-1 SAR image mosaic of Antarctica*. Alaska SAR Facility, Fairbanks, AK, in association with the National Snow and Ice Data Center, Boulder, CO. Digital media. http://nsidc.org/data/docs/daac/nsidc0103_ramp_mosaic.gd.html
- Jolliffe IT (2002) *Principal component analysis*, 2nd edn. Springer, New York
- Kärkäs E, Granberg HB, Kanto K, Rasmus K, Lavoie C and Leppäranta M (2002) Physical properties of the seasonal snow cover in Dronning Maud Land, East Antarctica. *Ann. Glaciol.*, **34**, 89–94 (doi: 10.3189/172756402781817554)
- King JC and Turner J (1997) *Antarctic meteorology and climatology*. Cambridge University Press, Cambridge
- Lehning M, Grünewald T and Schirmer M (2011) Mountain snow distribution governed by an altitudinal gradient and terrain roughness. *Geophys. Res. Lett.*, **38**(19), L19504 (doi: 10.1029/2011GL048927)
- Lemke P and 10 others (2007) Observations: changes in snow, ice and frozen ground. In Solomon S and 7 others eds. *Climate change 2007: the physical science basis. Contribution of Working Group I to the Fourth Assessment Report of the Intergovernmental Panel on Climate Change*. Cambridge University Press, Cambridge, 339–383
- Libbrecht KG (2005) The physics of snow crystals. *Rep. Progr. Phys.*, **68**(4), 855–895
- Liljequist GH (1957) *Energy exchange of an Antarctic snow-field. Surface inversions and turbulent heat transfer (Maudheim 71° 03' S, 10° 56' W)*. Norwegian–British–Swedish Antarctic Expedition, 1949–52, Scientific Results, Vol. 2, Pt I. Norsk Polarinstitutt, Oslo
- Matzl M and Schneebeli M (2006) Measuring specific surface area of snow by near-infrared photography. *J. Glaciol.*, **52**(179), 558–564 (doi: 10.3189/172756506781828412)
- Nagler T and Rott H (2000) Retrieval of wet snow by means of multitemporal SAR data. *IEEE Trans. Geosci. Remote Sens.*, **38**(2), 754–765 (doi: 10.1109/36.842004)
- Orheim O (1968) Surface snow metamorphosis on the Antarctic Plateau. *Nor. Polarinst. Arb.*, **1966**, 84–91
- Picard G, Arnaud L, Domine F and Fily M (2009) Determining snow specific surface area from near-infrared reflectance measurements: numerical study of the influence of grain shape. *Cold Reg. Sci. Technol.*, **56**(1), 10–17 (doi: 10.1016/j.coldregions.2008.10.001)
- Scambos TA, Haran TM, Fahnestock MA, Painter TH and Bohlander J (2007) MODIS-based Mosaic of Antarctica (MOA) datasets: continent-wide surface morphology and snow grain size. *Remote Sens. Environ.*, **111**(2–3), 242–257 (doi: 10.1016/j.rse.2006.12.020)
- Schlosser E, Manning KW, Powers JG, Duda MG, Birnbaum G and Fujita K (2010) Characteristics of high-precipitation events in Dronning Maud Land, Antarctica. *J. Geophys. Res.*, **115**(D14), D14107 (doi: 10.1029/2009JD013410)
- Schytt V (1958) *A. Snow studies at Maudheim. B. Snow studies inland. C. The inner structure of the ice shelf at Maudheim as shown by core drilling*. Glaciology II. Norwegian–British–Swedish Antarctic Expedition 1949–52, Scientific results, Vol. 4. Norsk Polarinstitutt, Oslo
- Shi J and Dozier J (2000) Estimation of snow water equivalence using SIR-C/X. Part II: inferring snow depth and particle size. *IEEE Trans. Geosci. Remote Sens.*, **38**(6), 2475–2487 (doi: 10.1109/36.885196)
- Sommerfeld RA and LaChapelle E (1970) The classification of snow metamorphism. *J. Glaciol.*, **9**(55), 3–17
- Stephenson PJ (1967) Some considerations of snow metamorphism in the Antarctic ice sheet in the light of ice crystal studies. In Oura H ed. *Physics of snow and ice*. Hokkaido University, Institute of Low Temperature Science, Sapporo, 725–740
- Ulaby FT and Dobson MC (1989) *Handbook of radar scattering statistics for terrain*. Artech House, Norwood, MA
- Van den Broeke MR, Reijmer CH, Van As D, Van de Wal RSW and Oerlemans J (2005) Seasonal cycles of Antarctic surface energy balance from automatic weather stations. *Ann. Glaciol.*, **41**, 131–139 (doi: 10.3189/172756405781813168)
- Wingham DJ, Shepherd A, Muir A and Marshall GJ (2006) Mass balance of the Antarctic ice sheet. *Philos. Trans. R. Soc. London, Ser. A*, **364**(1844), 1627–1635 (doi: 10.1098/rsta.2006.1792)
- Wiscombe WJ and Warren SG (1980) A model for the spectral albedo of snow. I. Pure snow. *J. Atmos. Sci.*, **37**(12), 2712–2733 (doi: 10.1175/1520-0469(1980)037<2712:AMFTSA>2.0.CO;2)
- Zwally HJ and 7 others (2005) Mass changes of the Greenland and Antarctic ice sheets and shelves and contributions to sea-level rise: 1992–2002. *J. Glaciol.*, **51**(175), 509–527 (doi: 10.3189/172756505781829007)